INTEK: Jurnal Penelitian
Vol. 13, No. 1, pp. 15-26, April 2026
DOI: https://doi.org/10.31963/intek.v13i1.5995

Development of a Current Signal Based Model for High Impedance Fault Identification in Power Systems

Andi Syarifuddin[1,*,a], Muhammad Nawir[2,b], Amelya Indah Pratiwi[2,c], and Hariani Ma'tang Pakka[2,d]
[1,2,3]Electrical Engineering Department, Universitas Muslim Indonesia, Jl. Urip Sumoharjo 5, Makassar, 90231, Indonesia

[*,a]asyarif@umi.ac.id (Corresponding Author), [b]muhammad.nawir@umi.ac.id, [c]amelyaindah.pratiwi@umi.ac.id, [d]hariani.m@umi.ac.id

Article Info

Keywords: High-impedance fault; correlation analysis; adaptive threshold; current signal processing; distribution protection

Received : 07 12 2025
Revised form : 31 03 2026
Accepted : 03 04 2026
Published : 25 04 2026

Abstract

High-impedance faults (HIFs) generate low-magnitude, highly irregular arc currents that closely resemble normal load behavior, causing conventio overcurrent-based protection to fail in their identification. This study proposes adaptive current-signal correlation model designed to detect HIFs using time-dom waveform similarity analysis. The method utilizes a band-pass filtered curr waveform, half-cycle window segmentation, and a correlation measurement agains reference pattern bank derived from varying ignition-angle scenarios. An adapt threshold mechanism is introduced to improve robustness against noise, switchi transients, and load fluctuations. The proposed model is validated throu MATLAB/Simulink simulations and Real-Time Digital Simulator (RTD experiments, representing near-real operating conditions of distribution feede Results demonstrate a detection accuracy of 97.69%, false alarm rate below 1.5%, a a detection time within one cycle (20 ms). Compared to harmonic, wavelet, and AN based methods, the proposed algorithm shows superior speed, computatio efficiency, and compatibility with existing current-based relay infrastructures. T approach enables practical field implementation without requiring additional sens or complex feature extraction.

1. Introduction

High impedance faults (HIFs) remain one of the most critical and challenging protection problems in electric power distribution systems. These faults typically occur when an energized conductor comes into contact with high-resistance surfaces such as dry soil, vegetation, or rigid ground materials, producing fault currents that are very small and often remain below the pickup level of conventional overcurrent relays [1], [2]. The inability of traditional protection schemes to identify HIF events in real time increases the risk of prolonged arcing, conductor ignition, equipment damage, and severe safety hazards for the public and surrounding environment [3]. As distribution systems continue to expand and carry increasingly diverse load characteristics, the demand for highly reliable HIF detection has become more urgent.

Conventional detection techniques frequently rely on harmonic distortion analysis, specifically exploiting even odd harmonic components to capture the nonlinear arcing attributes of HIF waveforms [4], [5]. Although these harmonic-based indicators are widely used, they are vulnerable to misclassification during inrush currents, capacitor switching, and nonlinear load variations, often resulting in high false-alarm rates. Other approaches utilize time frequency decomposition methods such as the Discrete Wavelet Transform (DWT) to extract transient fault features [6], [7]. While wavelet-based techniques can improve detection accuracy, their performance depends heavily on the selection of wavelet parameters and incurs high computational cost, making them less suitable for real-time protection in practical distribution feeders [8], [9].

Artificial intelligence (AI) methods such as Artificial Neural Networks (ANN), Support Vector Machines (SVM), Random Forests, and advanced deep-learning architectures have also been proposed to enhance HIF detection [10], [11], [12], [13], [14]. Although these methods show high classification performance, they require extensive training datasets, significant computational resources, and often lack interpretability and robustness when exposed to real-world disturbances. These drawbacks limit their applicability in protection systems that demand fast, deterministic, and transparent decision-making [15], [16].

Recent developments have introduced current-based fault location and protection algorithms that utilize data fusion, divergence detection, adaptive protection logic, and intelligent relaying for improving network reliability in the presence of renewable energy resources and inverter-based systems [17], [18], [19], [20]. Although these methods enhance general protection capabilities, the unique behavior of HIF signals low magnitude, intermittent arcing, and waveform irregularity remains inadequately addressed by most existing frameworks.

A promising alternative emerging in recent literature is time-domain correlation analysis of current waveforms, which evaluates the similarity between successive samples or compares the measured waveform with a reference HIF pattern bank [21],[22]. Correlation-based methods provide simpler implementation, reduced computational burden, and resilience against noise, enabling practical adoption in existing protection devices without requiring additional sensors. Some studies also indicate that correlation indicators can differentiate HIF events from non-fault phenomena such as load switching or transformer energization [23], [24]. However, previous correlation-based approaches are still constrained by their sensitivity to operating variations, lack of adaptive thresholds, and limited evaluation under complex distribution network scenarios.

Considering these limitations, this study proposes the development of an adaptive current-signal correlation model for HIF detection in medium-voltage distribution feeders. The proposed method improves upon existing correlation-based techniques by incorporating adaptive threshold optimization, precise digital filtering, and a dynamically constructed reference pattern bank derived from ignition-angle variations. The model is evaluated through comprehensive MATLAB/Simulink simulations and validated using Real-Time Digital Simulator (RTDS) experiments to represent near-real operating conditions. The algorithm is designed to operate using only current measurements, enabling direct integration into existing relay infrastructures without additional sensing hardware.

The contributions of this work are summarized as follows:

1. Development of a time-domain correlation model with adaptive thresholding for robust detection of HIF events under varying load and noise conditions.
2. Construction of a reference pattern bank representing wide-ranging arcing scenarios to enhance feature discrimination.
3. Integration of optimized signal filtering and sampling techniques for improved sensitivity and reduced false-alarm rates.
4. Validation through both simulation and RTDS data to ensure feasibility for real-time implementation in practical distribution systems.

The proposed approach addresses key gaps identified in state-of-the-art studies and supports the advancement of practical, cost-effective intelligent protection for modern power distribution networks.

2. Research Methodology

This research employs a current-signal–based detection framework for identifying high-impedance faults (HIFs) in distribution networks. The methodology consists of four main stages: (1) distribution system

modeling and HIF scenario construction, (2) current signal acquisition and preprocessing, (3) development of a time-domain correlation algorithm with adaptive thresholding, and (4) validation using MATLAB/Simulink and Real-Time Digital Simulator (RTDS) data.

2.1 Distribution System Modeling

A three-phase medium-voltage distribution feeder was modeled in MATLAB/Simulink to emulate normal operating conditions and various HIF scenarios. The system includes a 20 kV/0.4 kV transformer, linear and non-linear loads, capacitor banks, and multiple fault locations. HIFs were represented using time-varying impedances and arc characteristics for two surface conditions (600 Ω and 1200 Ω), capturing intermittent arcing behavior. The simulation produced high-resolution current-signal datasets for subsequent pattern-bank construction.

To provide a clear representation of the modeled system used in this study, the configuration of the medium-voltage distribution network is illustrated in Figure 1. The diagram highlights the main components of the system, including the power source, transformer, feeder structure, load types, and high-impedance fault (HIF) locations considered in the simulation.

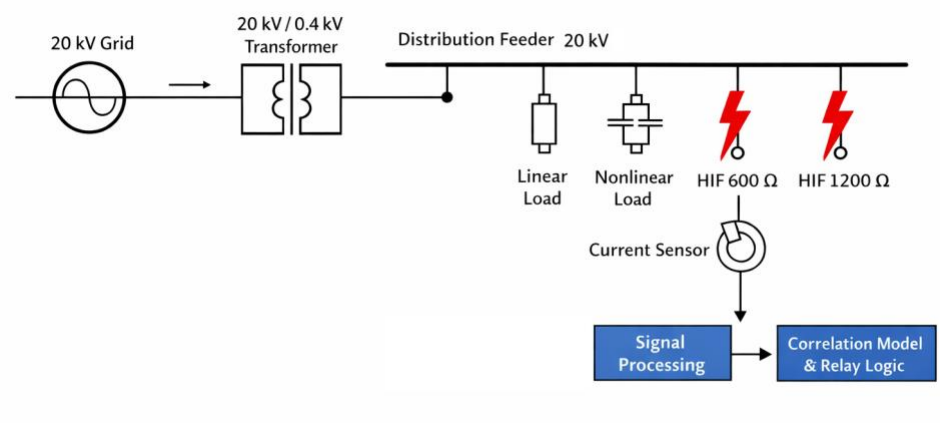

FIGURE 1. Modeled medium-voltage distribution system used for high-impedance fault (HIF)

As shown in Figure 1, the system consists of a 20 kV power grid connected to a step-down transformer (20 kV/0.4 kV), supplying a radial distribution feeder. The feeder includes multiple branches with linear and nonlinear loads, as well as a capacitor bank to represent reactive power compensation. High-impedance fault (HIF) scenarios are applied at selected locations using surface impedances of 600 Ω and 1200 Ω to emulate realistic fault conditions. Current measurements are captured through a sensor installed along the feeder and processed using the proposed correlation-based detection algorithm. This configuration enables comprehensive evaluation of the proposed method under various operating and fault conditions.

2.2 Current Signal Acquisition and Preprocessing

Current signals were obtained from two sources: MATLAB/Simulink simulations and RTDS experiments.

a. Digital Filtering

A fourth-order Butterworth band-pass filter (40–600 Hz) was applied to suppress DC offsets, low-frequency disturbances, and high-frequency switching noise while preserving fundamental and arcing-related waveform components.

To determine the most effective preprocessing strategy, several digital filtering techniques were evaluated under noisy operating conditions, as presented in Figure 2

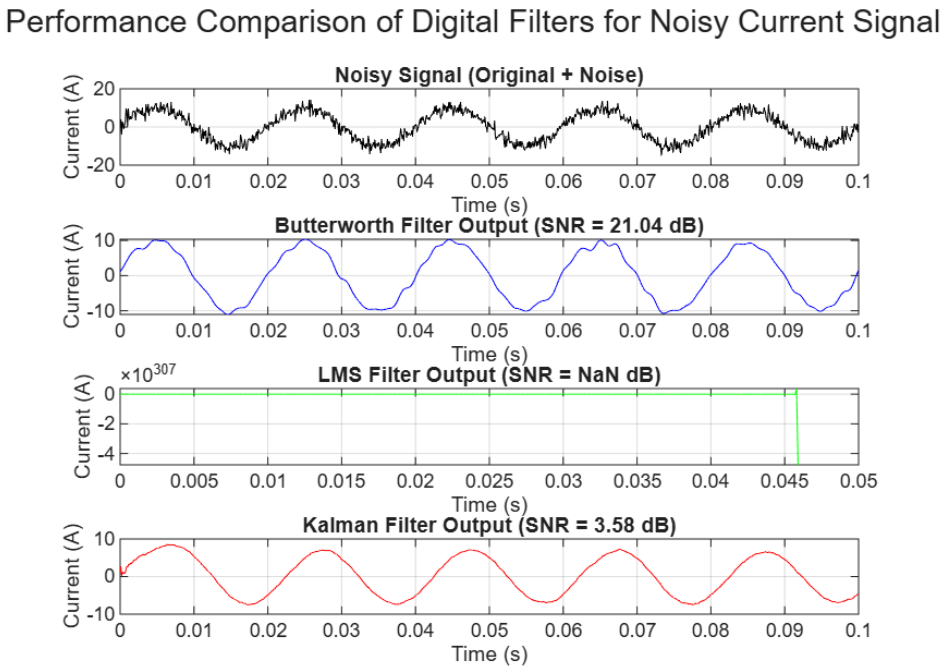

FIGURE 2. Comparison of digital filtering techniques for suppressing noise and switching transients in current signals

The Butterworth 40–600 Hz band-pass filter provides the smoothest waveform reconstruction while preserving HIF-related distortion components, outperforming the alternative filters in noise suppression and transient stability. This justifies its selection as the primary filtering method in the proposed algorithm.

b. Normalization

Signals were normalized using Z-score scaling to ensure consistent correlation computation across varying current amplitudes.

c. Sampling

A sampling rate of 12.8 kHz (256 samples per 50 Hz cycle) was used to capture fast arcing dynamics typically present in HIF waveforms.

2.3 HIF Pattern Bank Construction

A pattern bank consisting of 89 reference patterns was constructed from MATLAB/Simulink HIF simulations. Each pattern represents one cycle (20 ms) of current waveform corresponding to ignition angles

from 1° to 89° at 1° resolution. Each pattern contains 256 samples. This bank serves as a reference database for correlation-based matching.

2.4. Time-Domain Correlation Computation

Correlation coefficients were computed every half cycle (10 ms) using:

$$\rho = \frac{\sum_{k=1}^{N}(x_k - \bar{x})(y_k - \bar{y})}{\sqrt{\sum(x_k - \bar{x})^2}\sqrt{\sum(y_k - \bar{y})^2}} \quad (1)$$

where $x_k$is the measured current segment and $y_k$is the corresponding reference pattern from the pattern bank. Under normal conditions, consecutive waveform segments exhibit high similarity, whereas HIF-induced distortions reduce correlation values.

2.5. Adaptive Threshold Mechanism

An adaptive threshold scheme was developed to enhance discrimination between HIF and non-HIF transient events. Two thresholds were defined:

- Upper threshold (ρU): 0.45
- Lower threshold (ρL): 0.25

The threshold adapts to real-time variations in correlation values. Detection is triggered when correlation values exceed ρU within the defined window, while values between ρL and ρU are treated as a safety margin to prevent false alarms.

The optimization process for determining the adaptive lower and upper thresholds (ρL and ρU) under different load and noise conditions is shown in Figure 3.

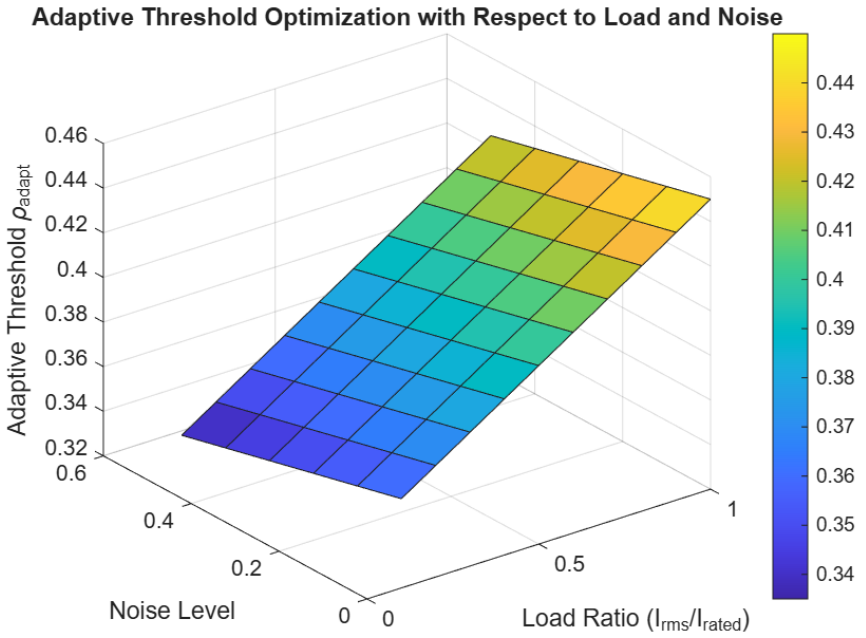

FIGURE 3. Adaptive threshold optimization showing the sensitivity of ρL and ρU under varying load and noise conditions

The figure demonstrates that setting ρL = 0.25 and ρU = 0.45 ensures reliable separation between HIF and non-HIF events across all evaluated conditions. This adaptive range effectively minimizes false alarms while maintaining high sensitivity, which is essential for real-time fault detection.

2.6. One-Cycle Detection Rule

RTDS measurements indicate that HIF correlation values rise sharply within the first 0.5–1 cycle. Accordingly, the detection logic was refined to a one-cycle decision rule: An HIF is declared when the correlation value exceeds ρU within one cycle (20 ms). This modification significantly reduces detection latency while maintaining reliable discrimination against non-HIF events.

2.7. Model Validation Using MATLAB and RTDS

The proposed model was validated through:

1. Simulated scenarios: normal loads, switching events, inrush currents, and HIFs with different impedances.
2. RTDS experiments: representing near-real distribution network conditions.

3. Results and Discussion

This section presents the results obtained from MATLAB simulations and RTDS experiments. Tables are interpreted in detail to highlight the model's performance and reliability.

3.1. Current Signal Characteristics

The fundamental differences between normal load currents and HIF-induced distortions are shown in Figure 4.

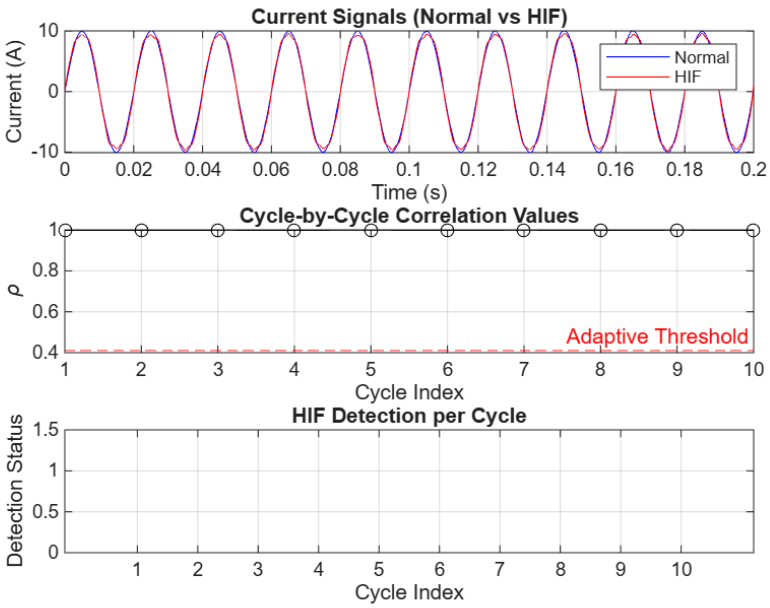

FIGURE 4. Comparison of normal and HIF current waveforms illustrating distortion and arc irregularities

The HIF waveform exhibits asymmetric irregularities, intermittent arcing, and reduced amplitude, clearly distinguishing it from the smooth sinusoidal pattern of normal operation.

These characteristics reinforce the suitability of correlation-based analysis for identifying HIF events. Table 1 summarizes the measured current characteristics under different operating conditions.

TABLE 1. Summary of Measured Current Characteristics

Condition	Phase A (A)	Phase B (A)	Phase C (A)	Description
Normal	42.3	41.9	42.1	Stable load
Inrush	112.5	41.0	42.0	Short-duration current surge
Switching	55.2	43.8	44.0	Short transient disturbance
HIF 600 Ω	16.8	41.7	42.0	Distorted waveform
HIF 1200 Ω	8.7	41.9	42.1	Very low fault current

HIF currents are significantly lower and exhibit irregular distortions compared to normal or switching conditions. These characteristics validate the need for correlation-based analysis instead of RMS or harmonic-based detection.

3.2. Noise Robustness Evaluation

Table 2 presents correlation values for non-HIF signals at various SNR levels.

TABLE 2. Correlation Values for Non-HIF Signals Under Different SNR Levels

SNR (dB)	Maximum Correlation
0	0.008
5	0.011
10	0.015
15	0.018
20	0.020

Normal signals consistently exhibit correlation values below 0.02, significantly lower than $\rho L = 0.25$. The filtering and preprocessing stages effectively suppress noise, demonstrating excellent noise immunity even under extreme conditions (SNR = 0 dB).

3.3. Correlation Response Under HIF Conditions

Table 3 shows the correlation behavior for HIF events at different SNR conditions.

TABLE 3. Correlation Levels for HIF Conditions at Various SNR Levels

SNR (dB)	Average Correlation
0	0.21
5	0.29
10	0.34
15	0.38
20	0.41

For SNR ≥ 5 dB, correlation values exceed the lower threshold ρL = 0.25. This demonstrates the proposed method's robustness and its ability to distinguish HIF distortions from noise-induced variations.

3.4. RTDS Half-Cycle Correlation Performance

Table 4 provides sample half-cycle correlation outputs obtained from RTDS experiments.

TABLE 4. Sample RTDS Half-Cycle Correlation Output

Half-cycle	Correlation	Decision
1	0.52	> ρU
2	0.57	> ρU
3	0.33	Safety margin
4	0.49	> ρU

Detection is achieved within a maximum of one cycle (20 ms), validating the effectiveness of the refined one-cycle detection rule. The pattern shows consistent correlation peaks during HIF events.

The real-time performance of the proposed adaptive correlation model was further validated using RTDS-generated current measurements, as illustrated in FIGURE 5.

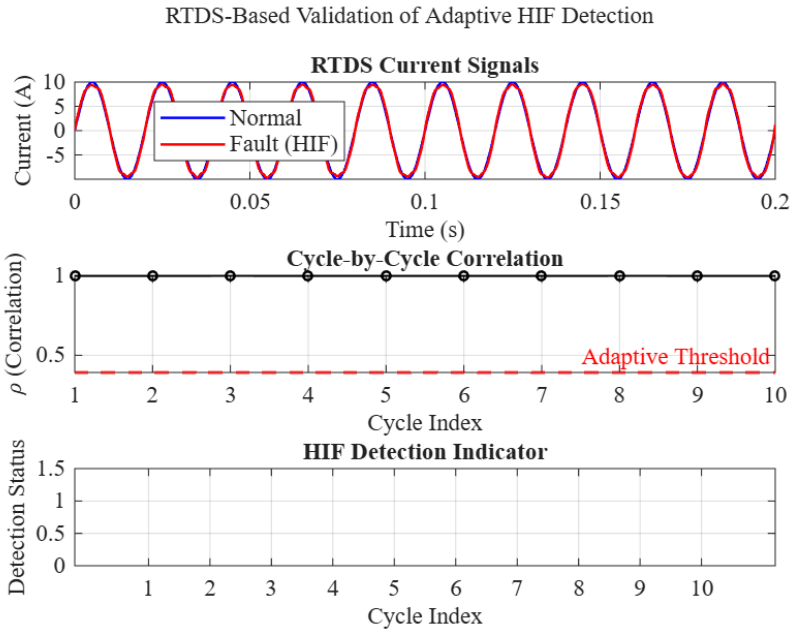

FIGURE 5. RTDS-based validation of the adaptive correlation model showing half-cycle correlation peaks during HIF conditions

As shown, the correlation values rise sharply above the upper threshold ρU during HIF events, enabling successful detection within one cycle, while non-fault intervals remain consistently below the decision boundary. These results confirm the robustness and real-time applicability of the proposed method under practical operating conditions.

3.5. Performance Comparison with Conventional Methods

Table 5 summarizes the performance comparison.

TABLE 5. Performance Comparison Between Proposed and Conventional Methods

Method	Accuracy (%)	False Alarm (%)	Detection Time	Noise Robustness
Proposed Correlation	97.69	<1.5	≤ 20 ms	Excellent
Harmonic-Based	88.2	12–18	40–60 ms	Weak
Wavelet (DWT)	92.5	7–10	30–50 ms	Moderate
ANN-Based	95.1	5–7	~40 ms	Depends on training

The proposed method outperforms conventional techniques in accuracy, detection speed, false alarm rate, and noise resilience. This highlights its practicality for real-time protection.

3.6. Overall Accuracy and Error Rates

Table 6 shows the accuracy based on simulation and RTDS datasets.

TABLE 6. Accuracy and Error Rates Across Different Datasets

Dataset	Accuracy (%)	False Alarm (%)	False Negative (%)
Simulation	98.3	2.1	1.7
RTDS A	97.8	2.4	2.2
RTDS B	97.9	2.0	2.1
RTDS C	98.1	1.8	1.9

Accuracy values are consistently high across all datasets, demonstrating stability, repeatability, and reliability of the proposed detection algorithm in both simulation and near-real conditions.

4. Conclusion

The study presented a current signal-based high-impedance fault (HIF) detection method employing time-domain correlation analysis with an adaptive thresholding mechanism. The proposed approach demonstrated fast detection capability, achieving reliable identification of HIF events within a single cycle (20 ms) through the refined one-cycle decision rule. Experimental results from MATLAB/Simulink and RTDS measurements confirmed strong noise resilience, as non-HIF signals consistently yielded correlation values below 0.02 across SNR levels ranging from 0 to 20 dB. The method also achieved high accuracy, with detection rates of 97.69–98.3% and false-alarm rates below 1.5%. Comparative evaluations further showed that the proposed algorithm outperforms harmonic-based, wavelet-based, and ANN-based techniques in terms of accuracy, detection

speed, and robustness under varying operating conditions. In addition to its performance advantages, the method requires only current measurements and is therefore compatible with existing distribution protection systems. Overall, the proposed scheme offers an effective, computationally lightweight, and practically implementable solution for reliable HIF detection in modern distribution networks, supporting seamless integration into real-time relay applications. Future work will focus on extending the model to multi-point measurement environments and evaluating performance under distributed energy resource (DER) penetration.

Acknowledgements

The authors would like to acknowledge the Institute for Research and Community Service (LP2S), Universitas Muslim Indonesia, for its financial support, which played an important role in enabling the completion of this research.

Data Availability Statement

The data that support the findings of this study are available on request from the corresponding author

Reference

[1] A. Syarifuddin, M. A. Masa, S. Syahrul, N. Nurul, and H. M. Pakka, "Enhanced detection of high impedance faults in smart distribution networks using differential energy indicators," *PROtek J. Ilm. Tek. Elektro*, vol. 12, no. 2, pp. 99–105, 2024.

[2] Y. Liu, Y. Zhao, L. Wang, C. Fang, B. Xie, and L. Cui, "High-impedance Fault Detection Method Based on Feature Extraction and Synchronous Data Divergence Discrimination in Distribution Networks," *J. Mod. Power Syst. Clean Energy*, vol. 11, no. 4, pp. 1235–1246, 2023, doi: 10.35833/MPCE.2021.000411.

[3] G. N. Lopes, T. S. Menezes, D. P. S. Gomes, and J. C. M. Vieira, "High Impedance Fault Location Methods: Review and Harmonic Selection-Based Analysis," *IEEE Open Access J. Power Energy*, vol. 10, no. September 2022, pp. 438–449, 2023, doi: 10.1109/OAJPE.2023.3244341.

[4] T. Treider and H. K. Høidalen, "Estimating distance to transient and restriking earth faults in high-impedance grounded, ring-operated distribution networks using current ratios," *Electr. Power Syst. Res.*, vol. 224, no. August, 2023, doi: 10.1016/j.epsr.2023.109765.

[5] T. A. Zerihun, T. Treider, H. Taxt, L. B. Nordevall, and T. S. Haugan, "Two novel current-based methods for locating earth faults in unearthed ring operating MV networks," *Electr. Power Syst. Res.*, vol. 213, no. July, 2022, doi: 10.1016/j.epsr.2022.108774.

[6] H. Liang, H. Li, and G. Wang, "A Single-Phase-to-Ground Fault Detection Method Based on the Ratio Fluctuation Coefficient of the Zero-Sequence Current and Voltage Differential in a Distribution Network," *IEEE Access*, vol. 11, no. January, pp. 7297–7308, 2023, doi: 10.1109/ACCESS.2023.3238072.

[7] M. J. B. B. Davi, M. Oleskovicz, and F. V. Lopes, "An impedance-multi-method-based fault location methodology for transmission lines connected to inverter-based resources," *Int. J. Electr. Power Energy Syst.*, vol. 154, no. August, 2023, doi: 10.1016/j.ijepes.2023.109466.

[8] J. G. An, J. U. Song, and Y. S. Oh, "A fuzzy-based fault section identification method using dynamic partial tree in distribution systems," *Int. J. Electr. Power Energy Syst.*, vol. 153, no. June, 2023, doi: 10.1016/j.ijepes.2023.109344.

[9] Y. Liang, A. He, J. Yuan, T. Wu, and Z. Jiao, "An accurate fault location method for distribution lines based on data fusion of outcomes from multiple algorithms," *Int. J. Electr. Power Energy Syst.*, vol. 153, no. January, 2023, doi: 10.1016/j.ijepes.2023.109290.

[10] J. Li *et al.*, "An adaptive protection scheme for multiple single-phase grounding faults in radial distribution networks with inverter-interfaced distributed generators," *Int. J. Electr. Power Energy Syst.*, vol. 152, no. September 2022, 2023, doi: 10.1016/j.ijepes.2023.109221.

[11] R. Xu, G. Song, Z. Chang, C. Zhang, J. Yang, and X. Yang, "A ground fault section location method based on active detection approach for non-effectively grounded DC distribution networks," *Int. J. Electr. Power Energy Syst.*, vol. 152, no. September 2022, 2023, doi: 10.1016/j.ijepes.2023.109174.

[12] X. Wang *et al.*, "Fault location based on variable mode decomposition and kurtosis calibration in distribution networks," *Int. J. Electr. Power Energy Syst.*, vol. 154, no. July 2022, pp. 1–10, 2023, doi: 10.1016/j.ijepes.2023.109463.

[13] M. Duan, Y. Liu, D. Lu, and R. Pan, "A novel noniterative single-ended fault location method with distributed parameter model for AC transmission lines," *Int. J. Electr. Power Energy Syst.*, vol. 153, no. July, 2023, doi: 10.1016/j.ijepes.2023.109358.

[14] H. Mirshekali, A. Keshavarz, R. Dashti, S. Hafezi, and H. R. Shaker, "Deep learning-based fault location framework in power distribution grids employing convolutional neural network based on capsule network," *Electr. Power Syst. Res.*, vol. 223, no. March, 2023, doi: 10.1016/j.epsr.2023.109529.

[15] A. Srivastava, L. A. Tuan, D. Steen, O. Carlson, O. Mansour, and D. Bijwaard, "Dynamic state estimation based transmission line protection scheme: Performance evaluation with different fault types and conditions," *Int. J. Electr. Power Energy Syst.*, vol. 148, no. January, 2023, doi: 10.1016/j.ijepes.2023.108994.

[16] M. Z. Yousaf, S. Khalid, M. F. Tahir, A. Tzes, and A. Raza, "A novel dc fault protection scheme based on intelligent network for meshed dc grids," *Int. J. Electr. Power Energy Syst.*, vol. 154, no. June, 2023, doi: 10.1016/j.ijepes.2023.109423.

[17] M. Rizwan, C. Gao, X. Yan, S. Ahmad, and M. Zaindin, "An approach to disparage the blindness of backup protection in grid connected renewable energy sources system by inducing artificial fault current," *Int. J. Electr. Power Energy Syst.*, vol. 153, no. August 2022, 2023, doi: 10.1016/j.ijepes.2023.109185.

[18] Y. Wang, Q. Cui, Y. Weng, D. Li, and W. Li, "Learning picturized and time-series data for fault location with renewable energy sources," *Int. J. Electr. Power Energy Syst.*, vol. 147, no. June 2022, 2023, doi: 10.1016/j.ijepes.2022.108853.

[19] B. Shang, G. Luo, M. Li, Y. Liu, and J. Hei, "Transfer learning-based fault location with small datasets in VSC-HVDC," *Int. J. Electr. Power Energy Syst.*, vol. 151, no. January, 2023, doi: 10.1016/j.ijepes.2023.109131.

[20] H. S. Samkari and B. K. Johnson, "Time-Domain Protection Scheme for Microgrids With Aggregated Inverter-Based Distributed Energy Resources," *IEEE Access*, vol. 11, no. December 2022, pp. 13232–13242, 2023, doi: 10.1109/ACCESS.2023.3242908.

[21] A. Syarifuddin, H. Ma, H. Eren, and A. S. Alghamdi, "Optimizing THD in Modified Multilevel Inverters with IoT-Integrated MPPT Systems for Enhanced Efficiency," vol. 16, no. 2, pp. 198–209, 2024.

[22] A. Basalamah, H. Ma, H. Eren, A. S. Alghamdi, K. Kamil, and S. Y. Hartono, "Jurnal Nasional Teknik Elektro Comparing MPPT Algorithms for Improved Partial-Shaded PV Power Generations," vol. 3, 2023.

[23] M. Zainuddin and A. I. Pratiwi, "Analisis pelepasan beban menggunakan under frekuensi relay (UFR) pada sistem transmisi Gardu Induk Gorontalo Baru 150 kV," *J. Electr.*, vol. 12, no. 2, pp. 100–105, 2023.

[24] A. I. Pratiwi and M. Asri, "Analisis tegangan tembus dan hidrofobisitas isolator nano komposit resin epoksi dan SiO2," *Jambura J. Electr. Electron. Eng.*, vol. 3, no. 2, pp. 89–93, 2022.